HHS Public Access

Author manuscript

Sci Transl Med. Author manuscript; available in PMC 2016 May 03.

Published in final edited form as:

Sci Transl Med. 2015 September 16; 7(305): 305ra145. doi:10.1126/scitranslmed.aac6589.

CT-guided injection of a TRPV1 agonist around dorsal root ganglia decreases pain transmission in swine

Jacob D. Brown[1], **Maythem Saeed**[1], **Loi Do**[1], **Joao Braz**[2], **Allan I. Basbaum**[2], **Michael J. Iadarola**[3], **David M. Wilson**[1], and **William P. Dillon**[1,*]

[1]Department of Radiology and Biomedical Imaging, University of California, San Francisco, San Francisco, CA 94117, USA

[2]Department of Anatomy, University of California, San Francisco, San Francisco, CA 94117, USA

[3]Department of Perioperative Medicine, Clinical Center, National Institutes of Health, Bethesda, MD 20892, USA

Abstract

One approach to analgesia is to block pain at the site of origin or along the peripheral pathway by selectively ablating pain-transmitting neurons or nerve terminals directly. The heat/capsaicin receptor (TRPV1) expressed by nociceptive neurons is a compelling target for selective interventional analgesia because it leaves somatosensory and proprioceptive neurons intact. Resiniferatoxin (RTX), like capsaicin, is a TRPV1 agonist but has greater potency. We combine RTX-mediated inactivation with the precision of computed tomography (CT)–guided delivery to ablate peripheral pain fibers in swine. Under CT guidance, RTX was delivered unilaterally around the lumbar dorsal root ganglia (DRG), and vehicle only was administered to the contralateral side. During a 4-week observation period, animals demonstrated delayed or absent withdrawal responses to infrared laser heat stimuli delivered to sensory dermatomes corresponding to DRG receiving RTX treatment. Motor function was unimpaired as assessed by disability scoring and gait analysis. In treated DRG, TRPV1 mRNA expression was reduced, as were nociceptive neuronal perikarya in ganglia and their nerve terminals in the ipsilateral dorsal horn. CT guidance to precisely deliver RTX to sites of peripheral pain transmission in swine may be an approach that could be tailored to block an array of clinical pain conditions in patients.

[*]Corresponding author. william.dillon@ucsf.edu.

SUPPLEMENTARY MATERIALS

www.sciencetranslationalmedicine.org/cgi/content/full/7/305/305ra145/DC1

Author contributions: J.D.B., D.M.W., and W.P.D. planned and performed the CT-guided injections and coordinated and oversaw the project. J.D.B., L.D., and M.S. performed animal behavioral experiments and animal dissection. A.I.B. and M.J.I. contributed to the experimental concept and design and data interpretation. J.D.B. and J.B. performed immunofluorescence analysis and qPCR. All authors contributed substantially to manuscript preparation and final approval of the version to be published.

Competing interests: M.J.I. is a co-inventor on a U.S. patent describing the use of intrathecal RTX for pain treatment. Patent #8,338,457, issued December 2012: “Selective ablation of pain-sensing neurons by administration of a vanilloid agonist.” The other authors declare that they have no competing interests.

INTRODUCTION

Poorly controlled pain can be incapacitating for patients and frustrating for health care providers. Despite decades searching for new pharmacologic modalities, there remain only a few categories of widely used medication (1, 2). Opioids continue to be effective for the treatment of severe pain but are often accompanied by debilitating central nervous system (CNS) side effects and addiction (3). Peripherally acting agents such as local anesthetics and corticosteroids are often limited by their nonselectivity and short duration of action. Procedures such as radio frequency ablation, usually targeting spinal facet arthropathy (degenerative joint disease between the articular processes of two adjacent vertebrae), provide longer pain relief in some patients but are not selective for pain fibers and can cause denervation of paraspinous musculature leading to atrophy and increased biomechanical strain (4). Ideally, the treatment of localized chronic pain would be accomplished by long-acting selective blockade of nociceptive neurons without affecting non-nociceptive sensory neurons and motor function, or causing adverse CNS side effects.

Recent approaches to new analgesics have targeted nociceptive sensory neurons by taking advantage of their unique molecular characteristics. One molecule of particular interest is the heat/capsaicin receptor TRPV1 (transient receptor potential cation channel, subfamily V, member 1), a ligand-gated cation channel with highly enriched expression in nociceptive C- and Aδ-fibers of the dorsal root and trigeminal ganglia (5). Neurons that express TRPV1 primarily transmit noxious heat or inflammatory pain sensations (6). TRPV1 is minimally expressed or absent in motor neurons and sensory pathways that transmit non-nociceptive information (for example, touch and proprioception) (6–10).

Resiniferatoxin (RTX) is an ultrapotent analog of capsaicin that occurs naturally in the latex of the cactus-like plant *Euphorbia resinifera* (11). RTX binds avidly to TRPV1-expressing nociceptive neurons and has been shown in animal and human dorsal root ganglia (DRG) neuron cultures to cause a rapid and prolonged influx of intracellular calcium ions. This potent response quickly compromises and then kills the TRPV1-expressing neurons (10, 12). These experiments provided important evidence that RTX selectively deletes TRPV1-expressing nociceptors in vivo.

Intrathecal and intraganglionic injections of RTX have a long-lasting effect due to permanent deletion of nociceptive cell bodies in the DRG or chemoaxotomy of the dorsal roots and nociceptive terminals in spinal cord (10, 13). Particularly relevant to the present study is that a single stereotactic microinjection of RTX into rat trigeminal ganglion produced a rapid (within 24 hours) blockade of C-fiber–mediated neurogenic inflammation and capsaicin-induced eye wipe responses, effects that lasted for at least 1 year (13). Intrathecal administration has also been used to treat intractable pain in advanced, naturally occurring canine osteosarcoma (14, 15) and is currently being investigated as a treatment for pain related to advanced cancer in a clinical trial at the National Institutes of Health (NIH) Clinical Center (16–18). Although an intrathecal approach may be warranted in patients with diffuse pain, the nonspecific anatomic delivery and possible cephalad dispersion of drug to cervical DRG or TRPV1-expressing neurons in rostral midbrain are limitations (17, 19).

A localized application targeting individual DRG has great advantages and can be tailored to treat many additional pain conditions. Computed tomography (CT) imaging allows the visualization and targeting of individual DRG and has evolved as an effective method to improve precision and safety during spinal interventions (20–22). Our results suggest that combining the high molecular selectivity of RTX pain blockade with the precision delivery of CT-guided injection may provide customizable therapy for a broad range of pain indications and body locations by directly targeting peripheral pain-transmitting neurons.

RESULTS

CT-guided periganglionic injection in pigs

We developed a modified transforaminal technique along the lumbar spine to access individual DRG with spinal needles in pigs (Fig. 1, A and B) (23). The goal was to distribute drug around the targeted DRG (that is, periganglionic) without accessing the intrathecal space or having the drug distribute in a contralateral fashion via the epidural space. We empirically determined that 275 μl (200 μl of drug or vehicle solution + 75 μl of contrast medium) was a minimum volume necessary to adequately coat the DRG. In each animal, we injected four ganglia on one side of the spine with either 500 ng (2.5 ng/μl, $n = 3$) or 2000 ng (10 ng/μl, $n = 4$) of RTX solution. The same four injected ganglia on the contralateral side received vehicle only. Bilateral injections were made to minimize the number of laboratory animals needed for this experiment, as well as to have an internal control for subsequent behavioral testing. The injection procedure was identical for both RTX and vehicle. Using CT imaging, we confirmed periganglionic distribution of solution immediately after injection (Fig. 1C). By obtaining a delayed scan at 10 to 15 min after injection, we also confirmed that any diffusion of drug/contrast away from the injection site was mild. We did occasionally observe thin layering within the ventral epidural space (4 of 56 injections) (fig. S1).

Disability scoring and gait analysis

Because the cytotoxic effects of RTX are receptor-mediated and limited to nociceptive neurons, we expected that treated animals would have no significant motor deficit or gait abnormality. To test this, we performed disability scores (based on a previous study at our institution) (24) for each animal for the first 3 days after injection and then once weekly over the next 4-week observation period (table S1). There was no evidence of lameness in any of the animals during this period (disability score = 0 for all seven animals). Separately, clinical gait scores were assessed using videography to record each animal as they were guided through a predetermined circuit before injection and during week 4 after injection. The animals were subsequently scored clinically according to a schema modified from the veterinary literature (25) (table S2). There was no abnormal gait observed in any of the animals before or after injection. Thus, each received a score of 1 (normal gait and walking). In addition, there were no observable differences in animal activity or diet between the animals injected with 500 ng RTX and those with 2000 ng RTX during this 4-week period, with mean weight gain of 13.4 ± 1.1 kg in the 500 ng RTX group and 13.3 ± 0.8 kg in the 2000 ng RTX group ($P = 0.93$).

C-fiber activation and behavioral analysis

On the basis of previous studies in small animal models (9, 13, 26), we expected that sensory dermatomes innervated by RTX-injected DRG would be less sensitive to nociceptive thermal stimuli when compared to the contralateral dermatomes injected with vehicle only. Our rationale for injecting four adjacent levels of the lumbar spine was to induce analgesia in a large enough area of the lateral hindlimb, which would allow for behavioral testing (Fig. 2A) (27, 28). We used an infrared diode laser, which does not contact the skin, to briefly and reproducibly activate the terminals of presumptive nociceptive afferents (6, 26, 29). We defined the withdrawal latency as the time in seconds from laser stimulation to a behavioral response, namely, skin twitch or limb withdrawal (movie S1). To test baseline response to the stimulus, we first activated C-fibers in the hindlimbs of uninjected control animals (n = 2) and evaluated the variability of the responses and left/right symmetry. We found no significant difference between withdrawal latencies of the two hindlimbs to repeated stimuli (P = 0.257; left, 6.2 ± 0.4 s; right, 6.5 ± 0.4 s; mean ± SEM) (Fig. 2B).

We first tested treated animals for behavioral responses at week 2 after injection and observed a statistically significant increase in withdrawal latency in both the 500 ng RTX (9.2 ± 0.3 s) and 2000 ng RTX (9.5 ± 0.3 s) groups, relative to the latency on the contralateral hindlimb (contralateral to 500 ng, 6.8 ± 0.4 s; contralateral to 2000 ng, 7.8 ± 0.3 s) (Fig. 2B). This corresponded to a 44.6 and 49.2% relative increase, respectively, compared to the uninjected control animals (6.3 ± 0.4 s). To test the durability of RTX-induced analgesia, we then repeated the laser stimulation in the same groups of animals 2 weeks later (4 weeks after the RTX injection) in an identical manner, with the exception that the stimulus cutoff was increased to 15.5 s (from 10.5 s at week 2) to make the test more stringent. At the earlier, 2-week time point, we used a lower cutoff because prolonged stimulation might produce skin damage, possibly confounding subsequent testing. We also reasoned that increasing the threshold at week 4 (the terminal study day) would allow better differentiation between the RTX and vehicle response. At week 4, we found that animals treated with 500 ng of RTX have a 115.2% increase in withdrawal latency (13.7 ± 0.5 s) relative to baseline latency in uninjected animals (6.3 ± 0.4 s) and a 46.4% increase relative to vehicle-injected contralateral dermatomes (9.3 ± 0.6 s; P = 0.0002) (Fig. 2C). In the animals treated with 2000 ng of RTX, we observed a 90.3% increase in mean withdrawal latency (12.1 ± 0.6 s) when compared to uninjected baseline (6.3 ± 0.4 s) and a 41.8% increase compared to the contralateral hindlimb (8.5 ± 0.4 s; P = 0.0003) (Fig. 2C). During the 4-week observation period, there were no skin ulcers observed within treated dermatomes or behavior suggestive of neuropathic itch.

Finally, it is of interest that in both dermatomes treated with 500 and 2000 ng of RTX, most trials at 2 and 4 weeks reached cutoff thresholds (500 ng, 60.7%, 37 of 61; 2000 ng, 59.6%, 53 of 89), but only a small percentage of trials on vehicle-injected dermatomes reached threshold (500 ng group, 15.7%, 11 of 70; 2000 ng group, 17.4%, 19 of 109) (Fig. 2D). We also noted that both vehicle- and RTX-injected dermatomes were sensitive to a noxious mechanical (pinprick) stimulus. However, we found the response rate highly variable, to the point that detailed conclusions, other than retention of pinprick sensitivity, could not be

drawn (movie S2). Individual response times to laser stimuli for all animals can be found in tabular format in the Supplementary Materials (table S3).

TRPV1 expression in RTX-treated DRG

We next wanted to verify on a molecular level that our image-guided intervention had deleted a significant proportion of TRPV1-expressing nociceptive neurons and to determine whether TRPV1 mRNA expression correlated with behavioral testing. As an initial test, we used quantitative polymerase chain reaction (qPCR) to compare mRNA transcripts in RTX-treated and untreated ganglia. Because separate injections were made at each DRG and the mean expression between pigs was similar (500 ng group, 57.8 to 68.4%; 2000 ng group, 29.1 to 37.6%), each DRG was treated independently for this analysis. The mean TRPV1 expression in DRG treated with 500 ng of RTX was reduced by 36.1 ± 7.3% (mean ± SEM) compared with control DRG. In DRG treated with 2000 ng of RTX, we observed a dose-dependent effect where TPRV1 mRNA expression was reduced by 66.3 ± 4.1% relative to control DRG (Fig. 3).

Immunofluorescence and histology in the DRG and dorsal horn

Consistent with the mechanism of action of RTX, we observed a decrease in markers of nociceptive cell bodies in the DRG and nerve terminals in the dorsal horn after treatment. The fraction of TRPV1-positive cell bodies in the RTX-treated ganglia (11.1 ± 1.6%, 140 of 1259 total cells) decreased by 66% relative to the contralateral ganglia (32.7 ± 3.4%, 476 of 1457; $P = 0.002$) (Fig. 4, A to C). To establish that another subset of sensory neurons remained intact, we examined expression of high–molecular weight neurofilament (NF200), a marker of a large proportion of myelinated neurons (30). The percentage of NF200-immunoreactive (IR) cell bodies was not significantly affected by RTX injection (RTX-treated DRG, 69.3 ± 3.9%, 567 of 818; vehicle-injected DRG, 71.6 ± 4.7%, 985 of 1375; $P = 0.27$), consistent with the receptor-based mechanism of action (Fig. 4, D to F). As a corollary to TRPV1 expression, we examined the fraction of cell bodies in DRG expressing substance P (SP), an excitatory neuropeptide often coexpressed in TRPV1-positive nociceptive cell bodies (31). SP-IR cell bodies in RTX-treated ganglia (10.7 ± 2.8%, 99 of 923) were decreased by 59% compared with contralateral ganglia (25.8 ± 2.7%, 418 of 1621; $P < 0.0001$) (Fig. 4, G to I). We also monitored calcitonin gene–related peptide (CGRP) immunoreactivity in the DRG and dorsal horn as CGRP defines a larger fraction of the nociceptors in DRG. Many DRG neurons coexpress TRPV1 (30). Consistent with this, the number of CGRP-IR cells decreased by 35.6% in treated DRG (27 ± 1.4%, 290 of 1055) compared to vehicle-only injection (42 ± 0.7%, 440 of 1044; $P = 0.005$) (Fig. 4, J to L). Quantitative fluorescence densitometry in the dorsal horn showed that there was a 40.8 ± 8.5% reduction in CGRP-IR terminals at the L5 segment on the RTX-treated side relative to the contralateral side (Fig. 4, M to O). Unfortunately, and consistent with literature reports, we found that currently available antibodies do not adequately detect TRPV1 immunoreactivity in the dorsal horn (30). However, the correlation between reduced CGRP-IR putative nociceptors in the DRG and terminals in the dorsal horn is indicative of a corresponding decrease of TRPV1-IR terminals in the dorsal horn.

We also compared vehicle- and RTX-injected DRG using traditional histology to evaluate whether we could directly visualize sequelae of the cell death and degeneration suggested by immunofluorescence. We observed a reduction in the overall number of ganglion cells and an increase in the number of intervening satellite cells in pig DRG treated with CT-guided injection of RTX compared to vehicle-injected DRG (Fig. 5). Additionally, in some foci, the satellite cells are seen forming small aggregates resembling the structures that have previously been described as nodules of Nageotte (Fig. 5D), defined as clusters of small basophilic cells arranged in rosette-like structures surrounding disintegrating neuronal bodies (13, 14, 32).

DISCUSSION

These results demonstrate that CT guidance can effectively target delivery of RTX directly to the DRG in a large mammal and produce lasting analgesia, providing proof of principle for RTX as an interventional, mechanism-based treatment. We demonstrate that RTX induces a cytotoxic effect on the TRPV1 subset of peripheral nociceptive neurons, diminishing the transmission of painful messages while leaving other sensory modalities in adjacent NF200-expressing myelinated neurons intact. The very specific molecular and cellular mechanisms of action highlight the potential use of RTX for the management of pain and support the results from previous studies (13–15, 17, 18). At the same time, we introduce an added dimension of anatomic selectivity by using the precision of image guidance to directly affect discrete yet critical loci in the sensory transmission pathway, potentially broadening the array of pain conditions that could be addressed by new selective analgesics and simultaneously narrowing the potential for anatomically off-target effects.

Our results showing that dermatomes innervated by RTX-treated DRG have a delayed or absent behavioral response to a noxious heat (laser) stimulus are consistent with the idea that there are fewer primary afferent neurons available to detect and transmit painful stimuli. Although both the 500- and 2000-ng doses of RTX are effective in reducing the response to the noxious heat stimulus, we did not detect a dose-dependent distinction in mean withdrawal time. This may be due to the relatively short time between limb withdrawal or lack thereof near the cutoff time and the onset of excessive tissue heating with potential skin damage beginning just after 15.5 s (cutoff week 4). This narrow window limits the discriminatory ability of the test and obscures our ability to detect true differences, if any, between RTX doses that may suppress withdrawal to more prolonged stimuli (6). It is also possible that both doses of RTX achieve a suprathreshold level of TRPV1-positive nerve deletion beyond which a test reliant on animal behavior cannot discriminate, that is, the remaining afferents do not relay enough of the painful message to stimulate a response. Recording electrophysiologic responses to a laser stimulus in an anesthetized animal, as previously done in mice, may provide a more sensitive correlation with TRPV1 afferent status (26), although this was outside the scope of our study.

As with other pain behavior tests in animal models, translating our results assumes a predictive relationship between noxious thermal sensation and the complex experience of pain. Although our approach is simplified, thermal sensitivity has proven to be a useful surrogate to predict responses to hypersensitivity and inflammatory pain models in a number

of species and has been correlated with clinical response to cancer-related pain (9, 13–15). We also have limited results showing that mechanical nociception, largely conveyed by a nonpeptidergic population of the Mrg family of G protein (heterotrimeric guanine nucleotide–binding protein)—coupled receptors, is not affected by TRPV1 ablation, as other studies have reported (8, 13, 26). However, we find behavioral testing methods that involve direct animal contact to be of limited use in a large, intelligent, and highly interactive animal, with spurious responses complicating interpretation. Although acknowledging the limitations of laser stimulus testing in our model, we find the relative advantages of this modality (no skin contact, reproducibility, predictive ability, and relative objectivity) compelling when compared with other pain behavior tests such as radiant heat sources and clinical or visual analogue scale–based scoring of inflammatory models of hyperalgesia (33, 34).

Because our experimental model relied on treating DRG corresponding to four adjacent vertebrae in one procedure, there was an increased risk of drug diffusion, such as we occasionally observed in the ventral epidural space, potentially leading to mild off target effects on the contralateral ganglia. Indeed, we observed a small but statistically significant increase in withdrawal latencies in vehicle-injected DRG in both the high- and low-dose groups. Although a mild, contralateral effect may be acceptable or suitable in some pain conditions, RTX administration could also be tailored to a unilateral pain condition. In such cases, injection could be made at only one or two adjacent DRG, or, for a multiganglionic treatment, staged over days to weeks, making the possibility of significant drug diffusion less likely.

One of the main limitations of this proof-of-principle study is the small sample size ($n = 7$ treated animals), which limits the ability to predict the true effect size if this approach were translated to a larger cohort. Additionally, although a pig provides a useful model for human anatomy and physiology, a large, intelligent animal presents significant challenges in terms of behavioral testing, and we found that traditional testing methods, such as pinprick stimulus, were prone to spurious response and artifact. We largely relied on noncontact, nociceptive thermal testing to assess for pain signaling and gait analysis for proprioception and musculoskeletal coordination but have not directly assessed other sensory modalities such as light touch, pressure, and vibration sense. Also, given the diversity of anatomic locations and physiologic systems expressing or innervated by TRPV1 fibers (pancreatic β islet cells, bladder, skeletal muscle, gastrointestinal tract, among others), it is possible that ablating TRPV1 fibers would have additional effects beyond nociceptive transmission in the peripheral nervous system, which can be evaluated further (30, 35–39). However, a highly localized method of delivery, such as what we report here, may help to mitigate unintended consequences. Finally, because our experimental design relied on using separate portions of each individual DRG for cellular (immunofluorescence and histology) and molecular (qPCR) assays, we were not able to directly quantify the absolute loss of neuronal cells in the entire treated DRG.

Our results provide a model for the type of approach that may be useful to alleviate localized neuropathic pain or pain from visceral organs such as the pancreas or kidney. Further studies may also establish the usefulness of fluoroscopic, CT-, or magnetic resonance–guided RTX

treatment tailored to a broader array of pain conditions including pain due to metastases, neuroma, localized nerve injuries, phantom limb pain, complex regional pain syndrome, osteoarthritis, radiculopathy, and trigeminal and postherpetic neuralgia. Treating peripheral pain generation directly with image-guided precision may advance the goal of selective pain medicine while reducing unwanted side effects, potentially offering a significant improvement on current strategies for controlling severe pain.

MATERIALS AND METHODS

Study design

This is a proof-of-principle study designed to assess the feasibility and efficacy of using image-guided delivery of RTX to induce selective analgesia in a large mammalian model. All protocols were approved by the University of California, San Francisco (UCSF) Institutional Animal Care and Use Committee (IACUC) conforming to the NIH animal care guidelines. A total of nine animals were used for this study: seven animals were injected with RTX or vehicle (500 ng per ganglion, $n = 3$; 2000 ng per ganglion, $n = 4$), and two animals were untreated. Interventionalists performing injections were aware of which DRGs were injected with RTX or vehicle, but subsequent data analyses regarding DRG treatment status were performed in a blinded fashion.

CT-guided injections

Female farm pigs (mean weight, 29.9 ± 0.4 kg) (Pork Power Farms) were premedicated with acepromazine (0.5 mg/kg; PromAce) and with ketamine (25 mg/kg) 30 min later (Ketaset) and anesthetized with a mixture of isoflurane 2 to 5% and oxygen. Vital signs (heart rate, electrocardiogram, respiratory rate, and O_2 saturation) were continuously monitored. A radiopaque marking grid was placed overlying the lumbosacral spine, and CT scan was performed with a 64-slice multiple detector CT scanner (LightSpeed Ultra, GE Healthcare) with the animals in the prone position (tube voltage, 140 kV; tube current, 120 to 250 mA; slice thickness, 1.25 mm). Spinal needles (9 cm, 22 G) were advanced under CT guidance to target the selected DRG, and drug or vehicle was administered to either the left or the right side. RTX preparations were made from a stock solution (100 μg/ml) from the NIH Clinical Center Pharmacy [in phosphate-buffered saline (PBS; pH 7.2), 0.05% ascorbic acid and 7% Tween 80] to a total concentration of 2.5 or 10 μg/ml. Injected volume consisted of 200 μl of RTX solution or vehicle combined with 75 μl of Omnipaque (240 mgI/ml) (iohexol) contrast medium (GE Healthcare) for a total volume of 275 μl infused via 1-ml syringes over 30 s. Postinjection CT scan was immediately obtained through the entire lumbar spine. We found inadequate covering of the DRG (drug was delivered too lateral) at two sites in each of three animals, and injections were repeated at these sites after needle tip was adjusted. Needles were then removed, and delayed CT images were obtained 15 min after injection.

Behavioral analysis

A disability score (range, 0 to 3) was assigned to each animal according to the scheme outlined (table S1). Animals were scored accordingly on each of the first 3 days after procedure and once weekly during weeks 2 to 4. Additionally, we used gait analysis by video recording animals that were walking spontaneously, before and after treatment (week

4), down the same corridor (12-m length), and observing gait distance, walking speed, limb support, and symmetry of movement. Accordingly, animals were assigned a clinical gait score (table S2).

C-fiber activation with laser stimulus

An infrared diode laser (DLD-20W; Lasmed) with an output wavelength of 980 nm was used to generate heat stimuli. Stepwise increases in laser current were administered to untreated pigs until a skin twitch or limb withdrawal was observed. A reproducible response was observed at 1400 mA, and this current was used in subsequent testing. A specialized testing enclosure was constructed on the basis of other studies (40, 41). Animals were fasted overnight and trained to enter this enclosure to obtain morning meal, allowing habituation before testing. Animals were released when they no longer showed interest in eating and began exploring the enclosure (15 to 25 min).

On the day of testing, the identical procedure was followed except that the laser stimulus was applied via fiber optic probe held at a distance of 20 to 60 cm from the skin surface (5-mm collimated laser beam delivers uniform energy within this range). A positive behavioral response was recorded when any of the following was observed: localized skin twitch, limb withdrawal, or rubbing limb against enclosure. After a positive response, the stimulus was immediately stopped, and withdrawal latency was recorded in seconds. If no response was observed, a preset cutoff automatically terminated the laser stimulus (10.5 s at week 2 and 15.5 s at week 4). Multiple stimulations (mean, 13.5 ± 1.2) were made within each group of dermatomes.

Response to a noxious mechanical stimulus was tested in treated animals 2 weeks after CT-guided injection. A pinprick stimulus was applied while the animal was within the same enclosure as previously described for laser testing. A clear skin twitch or limb withdrawal occurring almost immediately after stimulus application was considered a positive response.

Gene expression profiling with qPCR

Four weeks after the CT-guided injections, the pigs were killed, and the lumbar spinal cord and DRG were rapidly dissected. One half of each ganglion was used for qPCR analysis (the other half was used for anatomic studies). After disruption and homogenization, total RNA was isolated using the RNeasy Mini Kit (Qiagen) according to the manufacturer's protocol, and complementary DNA was synthesized using oligo(dT)s and Superscript III (Invitrogen) and briefly stored at −20°C. The mRNA levels for TRPV1 and β-actin were quantified with a CFX Connect real-time PCR system (Bio-Rad) using SYBR Green PCR Master Mix (Applied Biosystems). Three replicates were made for each ganglion. The following primers, spanning an intron, were designed using National Center for Biotechnology Information Primer-BLAST: (5′→3′): ACTB (GenBank, XM_003124280.3), forward, TCCACGAAACTACCTTCAACTC and reverse, AGCCATGCCAATCTCATCTC; TRPV1 (XM_005669121), forward, TCACCAACAAGAAGGGGCTC and reverse, GGATAGGTGCCTGCACTCAG.

Immunohistochemistry

Spinal cord and DRGs were rapidly dissected, and half the ganglion was immersion-fixed for 12 hours at 4°C in 4% paraformaldehyde, and then cryoprotected overnight in phosphate-buffered 30% sucrose. Tissues were frozen at −80°C in Tissue-Tek OCT (Finetek) and were cut at 25 (cord) or 16 μm (DRG). After 1-hour incubation in 10% normal goat serum in PBS with 0.3% Triton (NGST), the sections were incubated overnight in primary antibody solution diluted in 1% NGST. The following day, the sections were washed three times with 1% PBS and then incubated for 1 hour in secondary antibody (Alexa 488 or Alexa 594, 1:700 in 1% NGST). After washing three times in 0.1 M PBS, sections were coverslipped with Fluoromount-G (Southern Biotech). Primary antibodies included the following: rabbit anti-CGRP (1:1000; Peninsula), guinea pig anti-SP (1:1000, Invitrogen), chicken anti-TRPV1 (1:8000, Aves Labs), and mouse anti-NF200 (1:10,000, Sigma). Immunofluorescence densitometry was performed using ImageJ with a standardized region of interest applied to multiple cord sections. Manual cell quantification was performed using the Cell Counter plugin for ImageJ. H&E preparation was performed on 5-μm sections made from paraffin-embedded DRG.

Statistical analysis

Statistical analyses were performed using GraphPad Prism 6 software. Comparisons of withdrawal latency to multiple laser stimulus presentations were made between the left and right hindlimbs in untreated pigs using a Wilcoxon matched pairs signed-rank test ($\alpha = 0.05$, two-tailed P value). Analysis between vehicle- and RTX-injected dermatomes was made using a nonparametric Kruskal-Wallis test ($\alpha = 0.05$) with Dunn's posttest to correct for multiple comparisons. For qPCR, reactions were performed in triplicate and threshold cycle (C_T) data were analyzed with the $\Delta\Delta C_T$ method using β-actin as an internal standard. TRPV1 percent expression was compared using Wilcoxon matched pairs test ($\alpha = 0.05$, two-tailed P value). Cell quantification is a summation of DRG sections from three animals expressed as % IR cells per total cells counted.

Supplementary Material

Refer to Web version on PubMed Central for supplementary material.

Acknowledgments

We acknowledge the important contributions made to this project by M. Nemenov for consultation and training on the use of the laser device, M. Wilson and S. Hetts for their assistance with IACUC protocol preparation, C. Stillson for assistance with animal handling and anesthesia, S. Thompson for operating the CT scanner the during procedures, and D. Solomon, neuropathologist, for assisting in the histologic analysis of DRG samples.

Funding: This project was supported by grant funds from the Radiological Society of North America, Research and Education Foundation: RR1411 Resident Research Grant and Seed Grant #14-03 from the Department of Radiology and Biomedical Imaging, University of California, San Francisco, awarded to J.D.B. and W.P.D., and salary support for J.D.B. through the NIH T32 Postdoctoral Training Grant administered through the UCSF Department of Radiology. The contribution of A.I.B. and J.B. was supported by NIH DA29204 and NS14627. D.M.W. receives salary support through NIH R01 CA166766.

REFERENCES AND NOTES

1. Eddy NB, May EL. The search for a better analgesic. Science. 1973; 181:407–414. [PubMed: 4123997]
2. Meldrum ML. A capsule history of pain management. JAMA. 2003; 290:2470–2475. [PubMed: 14612484]
3. Foley KM. Opioids and chronic neuropathic pain. N Engl J Med. 2003; 348:1279–1281. [PubMed: 12660393]
4. Chou R, Atlas SJ, Stanos SP, Rosenquist RW. Nonsurgical interventional therapies for low back pain: A review of the evidence for an American Pain Society clinical practice guideline. Spine. 2009; 34:1078–1093. [PubMed: 19363456]
5. Goswami SC, Mishra SK, Maric D, Kaszas K, Gonnella GL, Clokie SJ, Kominsky HD, Gross JR, Keller JM, Mannes AJ, Hoon MA, Iadarola MJ. Molecular signatures of mouse TRPV1-lineage neurons revealed by RNA-seq transcriptome analysis. J Pain. 2014; 15:1338–1359. [PubMed: 25281809]
6. Mitchell K, Lebovitz EE, Keller JM, Mannes AJ, Nemenov MI, Iadarola MJ. Nociception and inflammatory hyperalgesia evaluated in rodents using infrared laser stimulation after *Trpv1* gene knockout or resiniferatoxin lesion. Pain. 2014; 155:733–745. [PubMed: 24434730]
7. Tender GC, Walbridge S, Olah Z, Karai L, Iadarola M, Oldfield EH, Lonser RR. Selective ablation of nociceptive neurons for elimination of hyperalgesia and neurogenic inflammation. J Neurosurg. 2005; 102:522–525. [PubMed: 15796388]
8. Basbaum AI, Bautista DM, Scherrer G, Julius D. Cellular and molecular mechanisms of pain. Cell. 2009; 139:267–284. [PubMed: 19837031]
9. Neubert JK, Karai L, Jun JH, Kim HS, Olah Z, Iadarola MJ. Peripherally induced resiniferatoxin analgesia. Pain. 2003; 104:219–228. [PubMed: 12855332]
10. Kárai LJ, Russell JT, Iadarola MJ, Oláh Z. Vanilloid receptor 1 regulates multiple calcium compartments and contributes to Ca^{2+}-induced Ca^{2+} release in sensory neurons. J Biol Chem. 2004; 279:16377–16387. [PubMed: 14963041]
11. Szallasi A, Blumberg PM. Resiniferatoxin, a phorbol-related diterpene, acts as an ultrapotent analog of capsaicin, the irritant constituent in red pepper. Neuroscience. 1989; 30:515–520. [PubMed: 2747924]
12. Olah Z, Szabo T, Karai L, Hough C, Fields RD, Caudle RM, Blumberg PM, Iadarola MJ. Ligand-induced dynamic membrane changes and cell deletion conferred by vanilloid receptor 1. J Biol Chem. 2001; 276:11021–11030. [PubMed: 11124944]
13. Karai L, Brown DC, Mannes AJ, Connelly ST, Brown J, Gandal M, Wellisch OM, Neubert JK, Olah Z, Iadarola MJ. Deletion of vanilloid receptor 1-expressing primary afferent neurons for pain control. J Clin Invest. 2004; 113:1344–1352. [PubMed: 15124026]
14. Brown DC, Iadarola MJ, Perkowski SZ, Erin H, Shofer F, Laszlo KJ, Olah Z, Mannes AJ. Physiologic and antinociceptive effects of intrathecal resiniferatoxin in a canine bone cancer model. Anesthesiology. 2005; 103:1052–1059. [PubMed: 16249680]
15. Brown DC, Agnello K, Iadarola MJ. Intrathecal resiniferatoxin in a dog model: Efficacy in bone cancer pain. Pain. 2015; 156:1018–1024. [PubMed: 25659068]
16. National Institute of Neurological Disorders and Stroke. Feb 12. 2015 http://clinicaltrials.gov
17. Amina Oughourli, FC.; Heiss, J.; Iadarola, M.; Smith, R.; Mannes, A. Pain and Quality of Life Assessments in Cancer Patients Pre and Post Intrathecal Resiniferatoxin Injection. Poster presented at the 39th Annual Regional Anesthesia and Acute Pain Meeting; Chicago, IL. April 2014;
18. Mannes A, Hughes M, Quezado Z, Berger A, Fojo T, Smith R, Butman J, Lonser R, Iadarola M. Resiniferatoxin, a potent TRPV1 agonist: Intrathecal administration to treat severe pain associated with advanced cancer—Case report. J Pain. 2010; 11:S43.
19. Cavanaugh DJ, Chesler AT, Bráz JM, Shah NM, Julius D, Basbaum AI. Restriction of transient receptor potential vanilloid-1 to the peptidergic subset of primary afferent neurons follows its developmental downregulation in nonpeptidergic neurons. J Neurosci. 2011; 31:10119–10127. [PubMed: 21752988]

20. Gangi A, Dietemann JL, Mortazavi R, Pfleger D, Kauff C, Roy C. CT-guided interventional procedures for pain management in the lumbosacral spine. Radiographics. 1998; 18:621–633. [PubMed: 9599387]
21. Silbergleit R, Mehta BA, Sanders WP, Talati SJ. Imaging-guided injection techniques with fluoroscopy and CT for spinal pain management 1. Radiographics. 2001; 21:927–939. [PubMed: 11452067]
22. Shepherd TM, Hess CP, Chin CT, Gould R, Dillon WP. Reducing patient radiation dose during CT-guided procedures: Demonstration in spinal injections for pain. AJNR Am J Neuroradiol. 2011; 32:1776–1782. [PubMed: 21920858]
23. Pleticha J, Maus TP, Christner JA, Marsh MP, Lee KH, Hooten WM, Beutler AS. Minimally invasive convection-enhanced delivery of biologics into dorsal root ganglia: Validation in the pig model and prospective modeling in humans: Technical note. J Neurosurg. 2014; 121:851–858. [PubMed: 24995785]
24. Bucknor MD, Rieke V, Do L, Majumdar S, Link TM, Saeed M. MRI-guided high-intensity focused ultrasound ablation of bone: Evaluation of acute findings with MR and CT imaging in a swine model. J Magn Reson Imaging. 2014; 40:1174–1180. [PubMed: 24925593]
25. Nganvongpanit K, Boonsri B, Sripratak T, Markmee P. Effects of one-time and two-time intra-articular injection of hyaluronic acid sodium salt after joint surgery in dogs. J Vet Sci. 2013; 14:215–222. [PubMed: 23814475]
26. Zhang J, Cavanaugh DJ, Nemenov MI, Basbaum AI. The modality-specific contribution of peptidergic and non-peptidergic nociceptors is manifest at the level of dorsal horn nociresponsive neurons. J Physiol. 2013; 591:1097–1110. [PubMed: 23266932]
27. Getty, R. The Anatomy of the Domestic Animals, Sisson and Grossman's. 5. W. B. Saunders Company; Philadelphia: 1975.
28. Terada K, Larson BJ, Owen JH, Sugioka Y. The effect of nerve root lesioning on various somatosensory evoked potentials in the hog. Spine. 1993; 18:1090–1095. [PubMed: 8367778]
29. Jiang, N.; Cooper, BY.; Nemenov, MI. Biomedical Optics (BiOS). International Society for Optics and Photonics; Bellingham, WA: 2007. p. 642809-642809-642808
30. Russo D, Clavenzani P, Sorteni C, Bo Minelli L, Botti M, Gazza F, Panu R, Ragionieri L, Chiocchetti R. Neurochemical features of boar lumbosacral dorsal root ganglion neurons and characterization of sensory neurons innervating the urinary bladder trigone. J Comp Neurol. 2013; 521:342–366. [PubMed: 22740069]
31. Price TJ, Flores CM. Critical evaluation of the colocalization between calcitonin gene-related peptide, substance P, transient receptor potential vanilloid subfamily type 1 immunoreactivities, and isolectin B_4 binding in primary afferent neurons of the rat and mouse. J Pain. 2007; 8:263–272. [PubMed: 17113352]
32. Jimenez-Andrade JM, Peters CM, Mejia NA, Ghilardi JR, Kuskowski MA, Mantyh PW. Sensory neurons and their supporting cells located in the trigeminal, thoracic and lumbar ganglia differentially express markers of injury following intravenous administration of paclitaxel in the rat. Neurosci Lett. 2006; 405:62–67. [PubMed: 16854522]
33. Mitchell K, Bates BD, Keller JM, Lopez M, Scholl L, Navarro J, Madian N, Haspel G, Nemenov MI, Iadarola MJ. Ablation of rat TRPV1-expressing Adelta/C-fibers with resiniferatoxin: Analysis of withdrawal behaviors, recovery of function and molecular correlates. Mol Pain. 2010; 6:94. [PubMed: 21167052]
34. Tzabazis A, Klyukinov M, Manering N, Nemenov MI, Shafer SL, Yeomans DC. Differential activation of trigeminal C or Aδ nociceptors by infrared diode laser in rats: Behavioral evidence. Brain Res. 2005; 1037:148–156. [PubMed: 15777763]
35. Akbar A, Yiangou Y, Facer P, Walters JR, Anand P, Ghosh S. Increased capsaicin receptor TRPV1-expressing sensory fibres in irritable bowel syndrome and their correlation with abdominal pain. Gut. 2008; 57:923–929. [PubMed: 18252749]
36. Ito N, Ruegg UT, Kudo A, Miyagoe-Suzuki Y, Takeda S. Activation of calcium signaling through Trpv1 by nNOS and peroxynitrite as a key trigger of skeletal muscle hypertrophy. Nat Med. 2013; 19:101–106. [PubMed: 23202294]

37. Akiba Y, Kato S, Katsube K, Nakamura M, Takeuchi K, Ishii H, Hibi T. Transient receptor potential vanilloid subfamily 1 expressed in pancreatic islet β cells modulates insulin secretion in rats. Biochem Biophys Res Commun. 2004; 321:219–225. [PubMed: 15358238]

38. Kindig AE, Heller TB, Kaufman MP. VR-1 receptor blockade attenuates the pressor response to capsaicin but has no effect on the pressor response to contraction in cats. Am J Physiol Heart Circ Physiol. 2005; 288:H1867–H1873. [PubMed: 15563536]

39. Light AR, Hughen RW, Zhang J, Rainier J, Liu Z, Lee J. Dorsal root ganglion neurons innervating skeletal muscle respond to physiological combinations of protons, ATP, and lactate mediated by ASIC, P2X, and TRPV1. J Neurophysiol. 2008; 100:1184–1201. [PubMed: 18509077]

40. Di Giminiani P, Petersen LJ, Herskin MS. Nociceptive responses to thermal and mechanical stimulations in awake pigs. Eur J Pain. 2013; 17:638–648. [PubMed: 23042703]

41. Di Giminiani P, Petersen LJ, Herskin MS. Characterization of nociceptive behavioural responses in the awake pig following UV–B-induced inflammation. Eur J Pain. 2014; 18:20–28. [PubMed: 23720380]

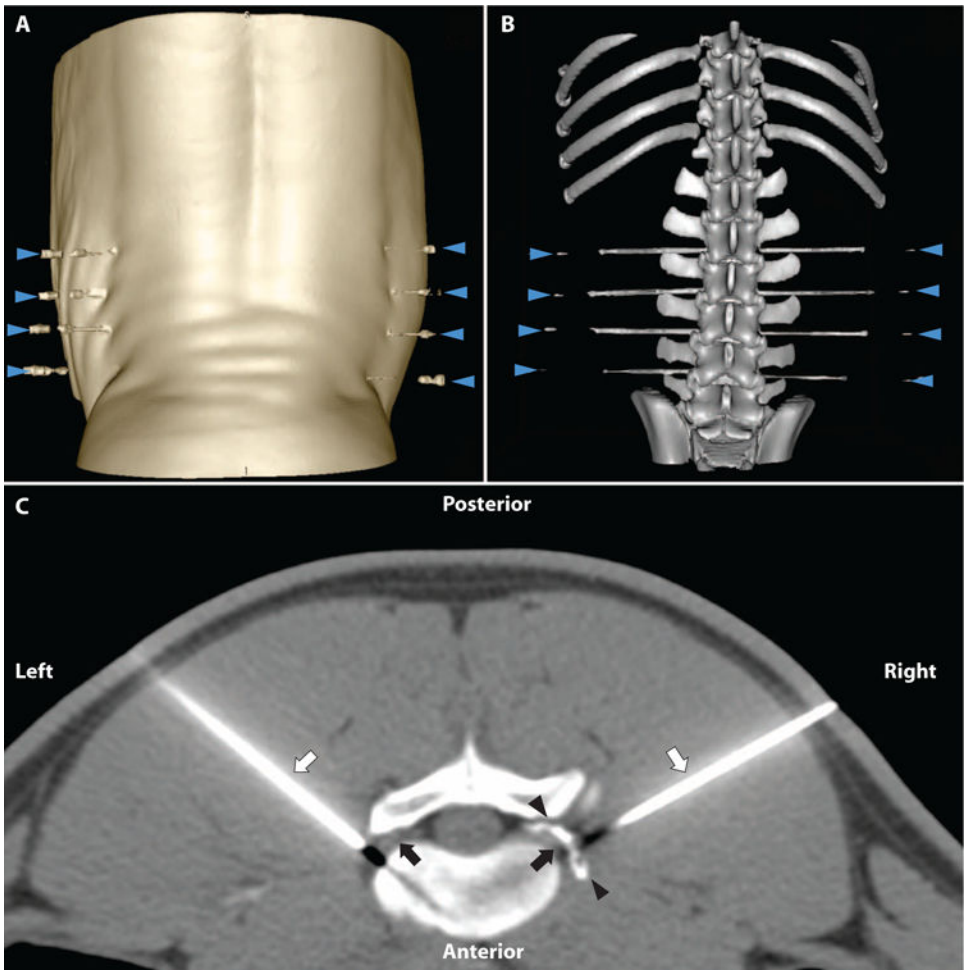

Fig. 1. CT-guided injections in a pig model

(**A**) Three-dimensional (3D) surface rendering of posterior skin surface with animal in prone position on CT table. Bilateral spinal needles are in place at the L2/3, L3/4, L4/5, and L5/6 levels (blue arrowheads). (**B**) In the same animal, 3D volume rendering of pig lumbosacral spine CT with spinal needles in place immediately adjacent to DRGs at the neuroforamina. (**C**) Axial CT image with pig in prone position. Scan obtained after injection of 2000 ng of RTX at the L4/L5 level. Periganglionic distribution of drug/contrast mixture is seen (black arrowheads) surrounding the exiting L4 DRG (black arrow) on the right (needle tip is out of plane of scan). Needle is in place to deliver vehicle solution (not yet injected) to left DRG. Black appearance distal to needle tip is a common CT artifact due to beam hardening along the needle path.

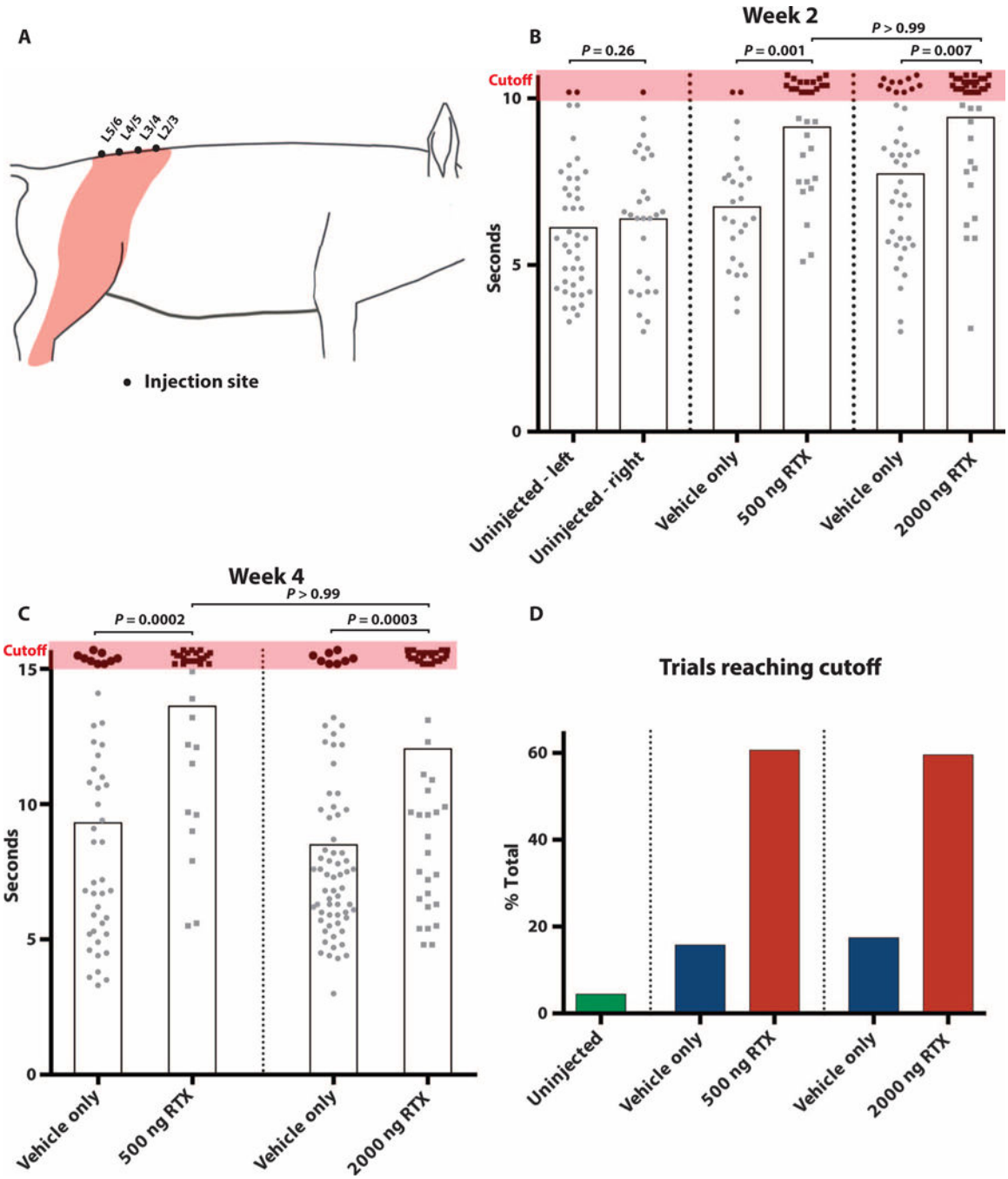

Fig. 2. Withdrawal latency to C-fiber activation with laser stimulus

(**A**) Diagram depicts the injected levels in pigs at L2/3, L3/4, L4/5, and L5/6, and the sensory dermatomes innervated by these ganglia (orange shading). C-fiber stimulations were confined to this shaded area. (**B**) Withdrawal latency at week 2 after injection with a 10.5-s cutoff threshold shows symmetric baseline withdrawal latency in uninjected animals. $n = 2$ ($P = 0.257$; left, 6.2 ± 0.4 s; right, 6.5 ± 0.4 s; 68 total stimuli). Significantly delayed or absent response in 500 ng (9.2 ± 0.3 s, $n = 2$) and 2000 ng (9.5 ± 0.3, $n = 3$) RTX groups relative to contralateral dermatomes injected with vehicle only (contralateral to 500 ng, 6.8

± 0.4; contralateral to 2000 ng, 7.8 ± 0.3). Data points reaching 10.5-s cutoff (orange shading) have been staggered slightly to minimize overlap. Individual stimuli, circle or square; mean response time, gray box. (**C**) Withdrawal latency at week 4 after injection with a 15.5-s cutoff. There is a significantly delayed or absent response in RTX-treated hindlimb (500 ng, 13.7 ± 0.5, $n = 3$; 2000 ng, 12.1 ± 0.6, $n = 4$) compared to the contralateral limb injected with vehicle only (500 ng, 9.3 ± 0.6; 2000 ng, 8.5 ± 0.4). (**D**) RTX-treated dermatomes have an increase in number of trials reaching cutoff (combined 2- and 4-week data): uninjected, 4.4% (3 of 68); 500 ng, 60.7% (37 of 61) versus vehicle control 15.7% (11 of 70); and 2000 ng, 59.6% (53 of 89) versus vehicle control 17.4% (19 of 109). Nonparametric Kruskal-Wallis test with Dunn's posttest to correct for multiple comparisons.

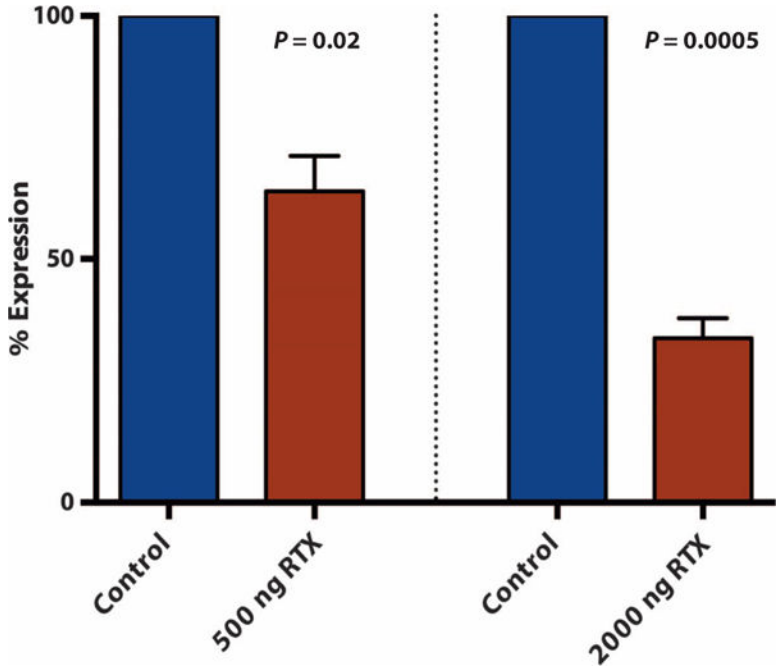

Fig. 3. Relative TRPV1 mRNA expression in treated DRG compared with control

Relative TRPV1 expression compared to control at the same lumbar level injected with 500 ng of RTX: 63.9 ± 7.3%, $n = 7$ DRG ($P = 0.02$), and with 2000 ng of RTX: 33.7 ± 4.1%, $n = 12$ DRG ($P = 0.0005$). Wilcoxon matched pairs test.

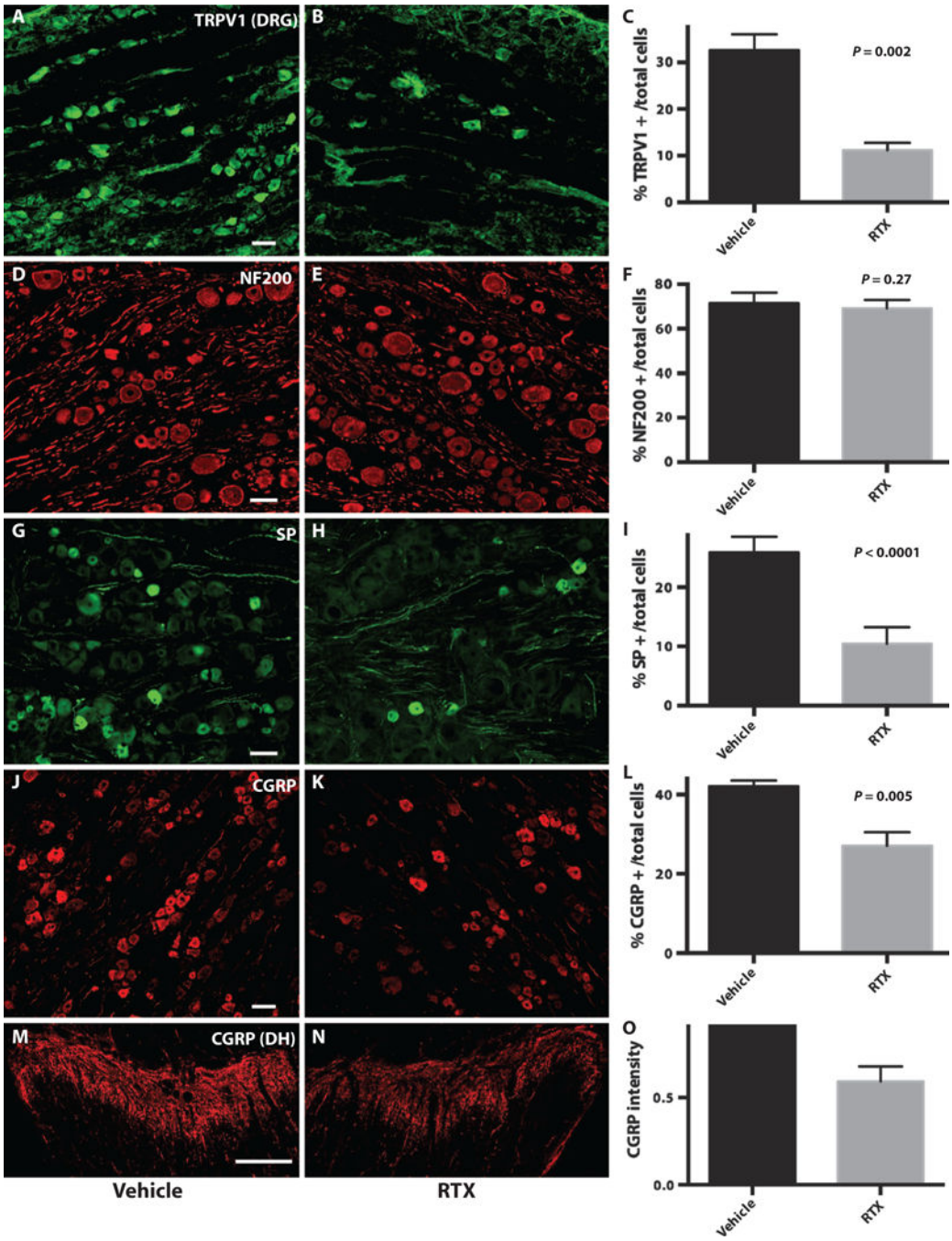

Fig. 4. Immunofluorescence in L4/5 DRG and nerve terminals in the spinal cord (L5)

(**A** to **C**) TRPV1 IR cell bodies from vehicle- (A) and RTX-injected (B) ganglia. (C) Bar graph depicts a 66% relative decrease in TRPV1 IR cells in RTX-treated (11.1 ± 1.6%, 140 of 1259) versus contralateral ganglia (32.7 ± 3.4%, 476 of 1457; $P = 0.002$). (**D** to **F**) NF200-IR cell bodies were not significantly affected by RTX injection (69.3 ± 3.9%, 567 of 818) (D); vehicle-injected DRG (71.6 ± 4.7%, 985 of 1375; $P = 0.27$) (E). (**G** to **I**) SP-IR cell bodies in RTX-treated ganglia (10.7 ± 2.8%, 99 of 923) (G) compared with contralateral ganglia (25.8 ± 2.7%, 418 of 1621) (H) were decreased by 59% ($P < 0.0001$). (**J** to **L**)

CGRP-IR cell bodies from vehicle-injected (27 ± 1.4%, 290 of 1055) (J) and RTX-injected (42 ± 0.7%, 440 of 1044; $P = 0.005$) (K) ganglia. (L) Bar graph depicts a 35.6% relative decrease. (**M** to **O**) CGRP-IR nerve terminals in the dorsal horn (DH) from vehicle- (M) and RTX-injected (N) sides of the same animal with a 40.8 ± 8.5% reduction (O) in CGRP nociceptive terminals. Cell counts are a summation of DRG sections from three animals and are expressed as % IR cells per total cells. Scale bars, 100 μm (A to K) and 300 μm (M and N).

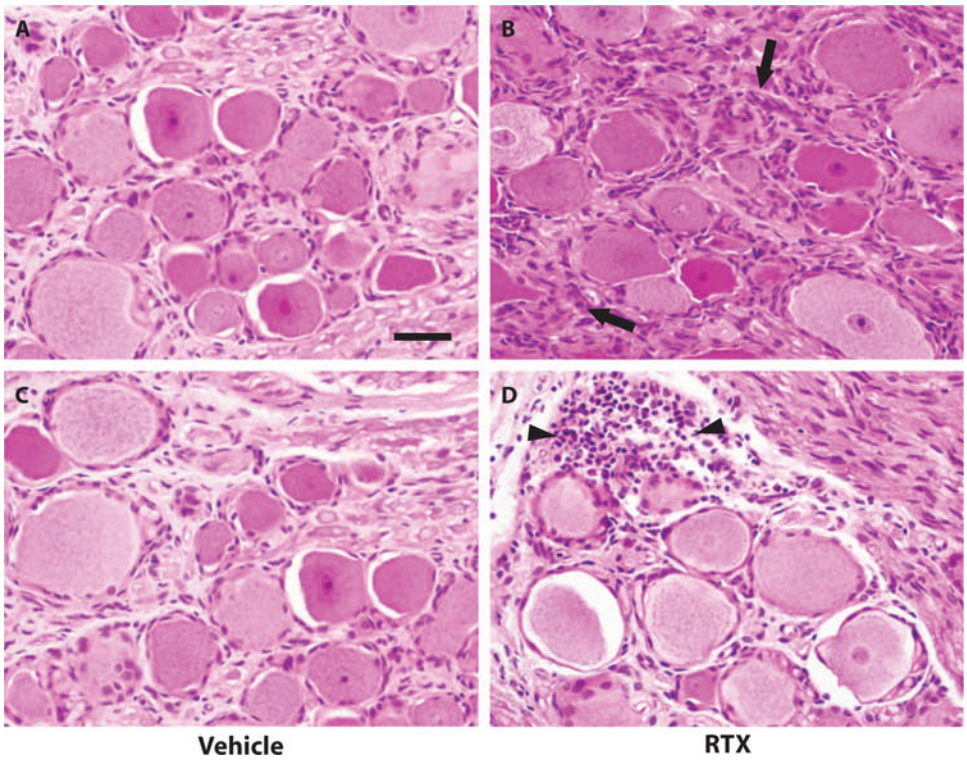

Fig. 5. Comparative histology of DRG injected with either vehicle or RTX

Hematoxylin and eosin (H&E) preparation of DRG parenchyma from lumbar DRG at ×40 magnification. (**A** and **C**) DRG injected with vehicle only demonstrating multiple large-, medium-, and small-diameter cell bodies with a generally thinly dispersed and uniform distribution of satellite cells, typically arrayed linearly along axons and in single cell layers around cell bodies. (**B** and **D**) In contrast, DRG injected with RTX demonstrate an overall reduction in the number of ganglion cells and an increase in the number of intervening, multilayered satellite cells (black arrows). Additionally, in some foci, the satellite cells are seen forming small aggregates resembling the structures that have been previously described as nodules of Nageotte (black arrowheads). Scale bar, 50 μm.